Journal of Physics: Conference Series **2885** (2024) 012027 doi:10.1088/1742-6596/2885/1/012027

Radiative heat transfer methodologies from compartment fires to adjacent walls: A Numerical Investigation

Angus Cameron[1], Eleni Asimakopoulou[2]

[1] University of Central Lancashire, Fylde Road, Preston, PR1 2HE, UK.
Angus.Cameron@kiwa.com
[2] University of Central Lancashire, Fylde Road, Preston, PR1 2HE, UK.
EAsimakopoulou@uclan.ac.uk

Abstract. In a fire scenario, the externally ventilating flames (EVF) often project beyond the compartment of fire origin and in some cases boundary distances, increasing the likelihood of fire spread between buildings. This work investigates various numerical methodologies to predict radiative heat transfer from compartment fires to adjacent walls at different orientations (20, 40, 60 and 80 degrees). Predictions were compared to empirically derived equations. Results show that code compliant scenarios may still exceed critical heat flux recommendations. Furthermore, the effects of prolonged heat exposure and materials should be considered by designers.

1. Introduction

Exterior fire spread has become an area of significant interest since the Grenfell Tower tragedy in 2017 [1] and external fire spread research has evolved significantly in the last decade [2]. Whilst engineers have focused attention on vertical flame spread, the risk of flame propagation between buildings is often less obvious. The recent fire in Valencia demonstrated how fires can spread between buildings [3]. Existing methods such as the BRE 187 methodology are widely used by engineers across the UK [4]. However, this approach is reliant on simplification and assumptions and therefore in some cases may not allow safe separation distances between buildings. This study aims to highlight possible approaches to improve our current methods for predicting radiative heat transfer.

1.1. Research On Externally Venting Flames (EVF)

Various researchers have derived empirical correlations that investigate externally venting flames (EVF). Law analyzed EVF thickness and width and found that the flame projects the entire length of the window and therefore could be simplified as a rectangular emitter. Law also determined that the horizontal flame projection (measured along the flame centerline to the tip of the flame) was dependent on the window aspect ratio. Depending on the window height and width, Law [5] found that the flame would react differently. The relationship between opening geometry and excess heat release rate (HRR) is widely accepted within fire engineering. McKeen and Liao [6] studied the coefficients derived from various authors' experimental research to predict horizontal flame projection. Other authors such as Lee, Delichatsios and Silcock [7] performed a series of experiments to investigate the lateral projection of plumes emerging from a ventilation-controlled compartment. These experiments showed that the external plume shape could be approximated by placing a rectangular fire source on the neutral plane. The characteristic lengths (l_1 and l_2) describe the shape of the plume outside the opening. It is also possible to represent the plume as a semi-circular fire source.

Since the 1940s, various authors have studied the effects of radiative heat transfer in order to predict safe separation distances between buildings. Notably, Lie [8] was one of the first authors to consider radiation intensity for different geometric angles in 1957. Lie examined radiation further, producing an improved 'heat balance' calculation method in 1967. The configuration factor method (CFM) assesses the fraction of radiation leaving one surface and arriving at another (i.e. the radiation between the emitting surface and

receiving surfaces). These factors are determined by the size, geometry, position, and orientation of the two surfaces. It is possible to derive expressions algebraically for different geometric configurations. However, more commonly predefined expressions are provided within literature [9]. This concept forms the basis for the BRE 187 methodology that is referenced by legislative guidance (Approved Document B) and has been deemed a satisfactory approach for determining safe separation distances [2][4]. The BRE 187 methodology suggests that a critical heat flux below 12.6kW/m^2 should be maintained to prevent pilot ignition. Furthermore, walls at an angle more than 80 degrees to the plane of reference can be discounted as it is assumed radiative intensity is sufficiently low [4].

To date, little focus has been placed on the methodology underlining legislative guidance. Consequently, it is possible for secondary ignition to occur due to prolonged heat exposure. This work investigates various numerical methodologies to predict radiative heat transfer from compartment fires to adjacent walls. Full-scale experiments conducted by Cheng and Hadjisophocleous [10] measured the heat flux received on a target wall for various window geometries and separation distances. This research was used to validate the developed numerical methodologies. This paper investigates the impact of altering the angle and target wall surface material, providing insight into the probability of secondary ignition for common façade materials.

2. Methodology

The heat flux and temperature distribution were predicted on the target wall for common wall materials (cement board, glass, wood, aluminium, and fibre insulating board). The materials selected have a range of properties and therefore would provide insight into how these walls would react when exposed to radiation in a code compliant design scenario. The orientation of the wall was also varied at 4 different angles (20, 40, 60 and 80 degrees). Numerical simulations using FDS version 6.8 (Fire Dynamic Simulator), Ansys Student R1:2023 (Transient Thermal) and Thermal Radiative Analysis (TRA) software packages were used to model each of the cases shown in Table 2. A schematic of the arrangement is presented in Figure 1. However, as FDS is limited by the numerical grid structure, the angled wall cases were not simulated in this software. The experimental and theoretical analysis performed by Cheng and Hadjisophocleous [10] allowed the results from the software packages to be analysed for the 180-degree façade scenario. These results were used to validate the assumptions for the EVF. Simulations were performed on twin CPU processors each with 1.70GHz and 60GB of RAM.

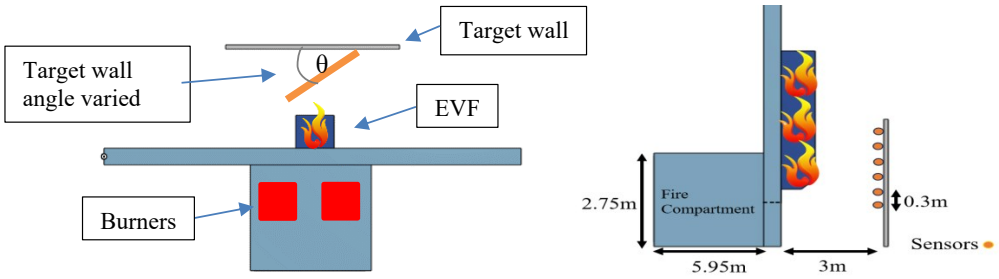

Figure 1 Top and side schematics of the numerical model of the fire compartment and target wall.

The FDS simulations followed the parameters shown in Cheng and Hadjisophocleous's study for the 1.45 m x 1.45 m opening scenario with the target wall at a distance of 3 m and 180 degree angle. The wood-framed target wall (4.88 m x 4.88 m) was initially constructed from non-combustible cement board. Thermocouples and radiometers were placed at 0.3 m intervals along the window centreline. The material properties were not referenced by Cheng and Hadjisophocleous. Nonetheless, data from literature was used which is shown in Table 1. It was assumed that the material properties were uniform, isotropic and homogeneous across their entire volume. The fire compartment geometry consisted of a 5.95 m x 4.4 m x 2.75 m with a 1.45 m x 1.45 m window, the opening was placed 1.095 m from the floor. The walls were well insulated with refectory insulating concrete. Thus, heat transfer losses were assumed minimal. Propane burners were used with a radiative fraction of 0.35 and soot yield of 0.05 [11]. A HRR of 5500kW was assigned to two 1 m x 1m burners that were placed 1m from the opening wall and 0.5 m from each of the side walls. The HRR value closely resembles figures presented in Dundar and Selamet's research for a modern living room fire [12]. A t^2 incipient growth rate was assumed. Burning was sustained for a 10-minute period, it was assumed that the fire was fully developed and limited by the air entrainment effect by this point. The

VLES model was used throughout this study. FDS applies a non-scattering grey gas model for the radiation and absorption coefficients [11]. While this simplification aids in solving the radiative transfer equation, it sacrifices accuracy. In certain situations, these factors can significantly impact the absorption and emission of thermal radiation. To account for the non-uniform distribution of radiative energy, the independent grid refinement study considered the number of radiative angles. In Case 1 the VLES and radiation transport equation (RTE) were set with 100 angles. In Case 2 the radiative angles were doubled, this significantly increased processing times. A grid resolution of 10 cm was used for a total of ~298,000 cells.

Table 1 Material thermal properties

Material	Density (kg/m^3)	Specific heat (J/kgK)	Thermal conductivity (W/mK)
Cement board [13]	1860	800	0.720
Glass [14]	2500	750	1.4
Wood [13]	700	2800	0.17
Aluminium [13]	2689	951	237.5
Fiber insulating board [13]	100	2000	0.04
Refectory insulating concrete [9]	1050	837	0.250

The Ansys simulations also followed the experimental parameters described previously. Ansys uses a surface-to-surface model (S2S) to predict radiative heat transfer. The incident radiation arriving on the materials surface is computed similarly to the CFM described in the literature review. However, Ansys considers an additional term for transient heat conduction that varies over the heating period. If a material is supplied with enough energy, steady-state conditions are reached. In these instances, the material can no longer store energy and instead acts as a thermally thin solid. The primary assumption of this model is the disregard of any absorption, emission, or scattering radiation. Furthermore, when there are many radiating surfaces this model can become increasingly complex to solve. In these cases, software packages adopt a clustering approach, whereby the temperature on adjoining surfaces are averaged. Ansys also has additional mesh optimisation tools. As computational resources were limited, a 12 cm cell size was selected to produce a structured mesh. Whilst this mesh size is larger than that used in the FDS study, this provided additional insight between case running times (as shown in Table 2). The front surface of the plume was averaged across its entire height, aligning with the S2S clustering approach discussed previously. A grid sensitivity study was performed on Ansys and FDS simulations to examine these results.

Table 2 Simulation descriptions

	Target Wall Orientation	Method	Radiation Model	Approx. Running Time
Case- 1	180 degrees	FDS	RTE with 100 angles	Long (1 week)
Case- 2	180 degrees	FDS	RTE with 200 angles	Long (2.5 weeks)
Case- 3	180 degrees	Ansys	S2S	Medium (1 day)
Case- 4	180 degrees	TRA	CFM	Short (5 minutes)
Case- 5	20 degrees	Ansys	S2S	Medium (1 day)
Case- 6	20 degrees	TRA	CFM	Short (5 minutes)
Case- 7	40 degrees	Ansys	S2S	Medium (1 day)
Case- 8	40 degrees	TRA	CFM	Short (5 minutes)
Case- 9	60 degrees	Ansys	S2S	Medium (1 day)
Case- 10	60 degrees	TRA	CFM	Short (5 minutes)
Case- 11	80 degrees	Ansys	S2S	Medium (1 day)
Case- 12	80 degrees	TRA	CFM	Short (5 minutes)

The TRA software is explicitly designed for predicting radiation between surfaces, this model solves the CFM equation discussed above [15]. However, in some situations, calculating the associated view factors for angled surfaces can be complex and error prone, this package is particularly useful to quickly estimate the radiation experienced on surfaces in such situations. As both the TRA and Ansys software packages do not solve the governing equations for fluid flows the plume geometry was user specified. As Law's work serves as the cornerstone for the BRE 187 methodology and Eurocode1 standard [5][16][17], the plume regions were approximated using equations referenced in these standards. An average plume temperature of 850ºC was

assumed for the front face of the plume in both the Ansys and TRA software packages, this value was based on the experimental measurements undertaken by Cheng and Hadjisophocleous' s [10]. The panel emitted heat at a constant rate in each of these simulations. Blackbody radiation was assumed in alignment with PD 7974 [18]. Notably, as gas flows from the opening a portion of heat is lost due to convection, this is accounted for in both FDS and Ansys but not TRA. PD 7974 recommends a figure of 4 kw/m^2 or 9 kw/m^2 [17]. The material properties and target wall orientation were varied once the fire model was verified. It was assumed that the target wall would not vary the air entrainment of the plume. All the cases modelled would be permissible under the BRE 187 methodology.

3. Results

Various authors have researched methods for predicting the height and horizontal projection of the EVF. The predicted parameters are shown in Table 3, the values were compared against the experimental study [10]. Due to the limited coloration between the fuel surfaces and pyrolysis of combustibles that occurs at the window, the theoretical calculations generally overpredict the flame height. These results suggest the flame would extend close to the top of the target wall. As shown in the experimental work, a wider window resulted in higher compartment temperatures due to increased air entrainment. Consequently, lower flame heights were observed as the unburnt hydrocarbons escape via the window opening and burn outside the compartment. Law's equation underpredicted the extension width by 4% compared to the experimental study [10].

Table 3 Plume height and lateral projection

Ref	EVF Height (H_f)	EVF Width (H_w)	Error (H_f)	Error (H_w)
Cheng and Hadjisophocleous [10]	3m	0.97m	-	-
Law (modelled in Ansys and TRA) [5]	4.1m	0.93m	26.83%	4.30%
Tang [19]	3.45m	-	13.04%	-
Goble [20]	3.09m	-	2.91%	-
Hu [21]	3.39m	-	11.50%	-
Cul [22]	4.93m	-	39.14%	-
FDS	4.0m	0.99m	14.3%	2.02%
Lee, Delichatsios and Silcock [7]	-	1.16m	-	16.38

Table 4 Peak heat flux on 180-degree wall

	Peak HF on target wall (kw/m^2)	Convection considered	Peak HF with convection (4kw/ m^2)	Error
Law [5]	24.12	no	20.12	9%
Tang [18]	22.31	no	18.31	1%
Goble [19]	21.04	no	17.04	7%
Hu [20]	22.11	no	18.11	1%
Cul [21]	25.75	no	21.75	16%
Case 1	18.14	yes	Considered in solver	0%
Case 2	17.73	yes	Considered in solver	3%
Case 3	15.97	yes	Considered in solver	14%
Case 4	18.32	no	14.32	14%
Experiment [10]	18.22	-	-	-

The results presented in Table 4 were comparatively compared against the experimental data to understand the accuracy of the numerical models. Cases 1 and 2 closely predicted the peak heat flux but both these cases took considerably longer to simulate (between 1 and 2.5 weeks). It was also noted that increasing the radiative angle had very little effect on the maximum heat flux. Whilst Cases 3 and 4 took significantly less time to solve, larger deviations between the experimental case were witnessed (14%). As both these cases solve the radiative heat transport equation in a similar manner, the results closely aligned when convective heat losses were considered (a difference of ~1.7kW/m^2 was observed between these cases). In comparison, the empirical equations overpredicted the heat flux observed in the experimental study, these deviations ranged between 13% and 24%. When convective heat losses were considered, this reduced between 1% and 16%. The heat flux errors observed in Cases 3 and 4 are possibly due to differences in the plume geometry. In all cases the

predicted heat flux exceeded the 12.5kW/m^2 threshold specified in guidance. Nevertheless, the arrangement would still comply with the enclosing rectangle methodology.

3.1. Varying Wall Angle and Materials

To compare the incident heat fluxes for Cases 3 and 4, convective heat losses of 4kW/m^2 were assumed. The 180-degree wall scenario received the most amount of radiative heat. The incident threshold criteria (12.6kw/m^2) was not met for the walls orientated at 20, 40, 60 and 80 degrees. As shown in Figure 2, the heat flux exponentially reduces as the wall angle is increased. Cases 11 and 12 showed peak heat fluxes ~3kW/m^2. Even when lower amounts of incident heat flux are experienced, some of the target specimens (fibre insulating board and glass) reached constant temperatures at 170s and 50s retrospectively. The reflective component is negligible for most of the materials. An exception to this was the glass specimen where the absorbed radiation was significantly lower than materials such as aluminium. Despite this, prolonged heat exposure also resulted in large temperature rises in the region of several hundred degrees for most of the cases simulated (the only exception was the Ansys simulation modelling aluminium). The results were close to those observed in the experimental study.

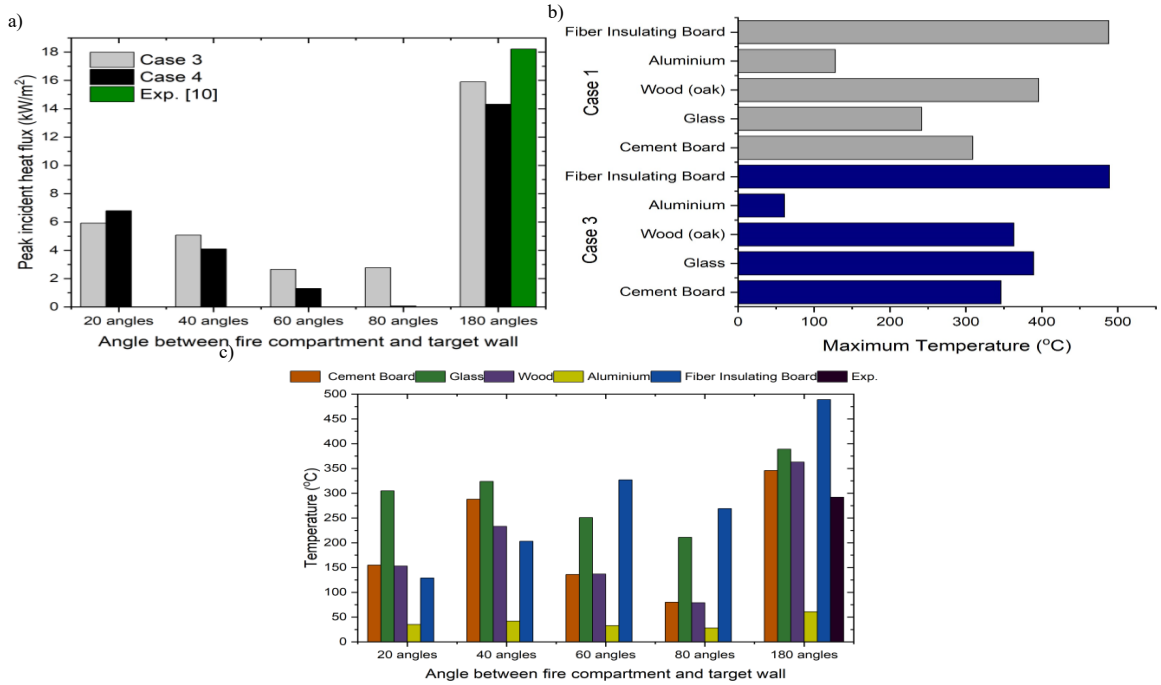

Figure 2 (a) Incident radiation (b) Maximum temperature comparison between models (180^0 wall) (c) Temperature comparison

BRE 187 suggests glass failure at temperatures ~200^{0}C [16]. Thus, the glass is expected to fail in all cases tested. Other materials such as the fibre insulation remained close to the ignition temperature for the orientated wall scenarios (335^{0}C) [23]. However, these materials are unlikely to be directly exposed to heat unless encapsulating materials fail. Aluminium alloys may fail due to thermal expansion in temperatures as low as 70^{0}C [24]. It is therefore possible that the aluminium would fail in the 180-degree scenario, the angled scenarios were near to this threshold. The cement board is unlikley to fail due to high ignition temperatures. These results also highlight the effect of prolonged heat exposure that may also result in failure. Figure 2 shows the difference between the user specified model, CFD simulations and experiment. Temperature was well predicted in Case 3 despite the simplifications made to the model. The fibre insulation cases were predicted within 1^{0}C. The peak temperatures were well approximated for the wood and cement board specimens (a difference ~35^{0}C was observed). The largest discrepancies were observed for the glass and aluminium samples (67^{0}C and 146^{0}C). When the average temperatures on the glass surface were considered, the results more closely aligned (within 30^{0}C). All materials (except aluminium) exceeded the characteristic temperature rise function shown in literature [23]. This function predicts a temperature rise between 200^{0}C-300^{0}C for thermally thick and thin materials under the incident heat flux conditions described in Table 4.

4. Conclusion

This study demonstrates how in certain scenarios the critical heat flux limits set in industry guidance may be breached for a code compliant scenario. In some situations, designers may wish to consider the contribution from the EVF rather than the rectangular window emitter, as the EVF can contribute a large amount of heat that can extend close to the boundary line and neighbouring compartments. This is currently not considered in current engineering practice. Furthermore, designers should also consider the target wall material and its orientation as failure may occur for certain materials (such as glass) at an angle greater than 80 degrees. This is currently not captured in current methods for predicting separation distances. This research maintains a separation distance of 3m, if the target wall is moved closer, increased heat flux and associated temperatures are assumed. Thus, designers may wish to orientate walls in their designs to reduce the incident heat flux. This observation could be applied to informal settlement buildings to reduce the likelihood of fire spread.

References

[1] M. Bonner, W. Wegrzynski, B. K. Papis and G. Rein, "KRESNIK: A top-down, statistical approach to understand the fire performance of building facades using standard test data," Build. Environ., vol. 169, pp. 106540, 2020.
[2] *The Building Regulations 2010. Approved Document B, Fire Safety. Volume 1, Dwellinghouses: Coming into Effect April 2007.* (2006th ed.) London: NBS, 2013.
[3] T. Symonds,"Valencia fire:Grenfell-style cladding fear after blaze,"05/03/24.Watford:BRE Press,2014.
[5] M. Law, *Some Selected Papers: Engineering Fire Safety.* London: Arup, 2002.
[6] P. Mckeen and Z. Liao, "The impact of horizontal projections on lateral fire spread in multi-unit residential buildings - comparison of numerical and similarity correlations," *Fire Saf. J.,* vol. 126, pp. 103441, 2021.
[7] Y. Lee, M. A. Delichatsios and G. W. H. Silcock, "Heat fluxes and flame heights in façades from fires in enclosures of varying geometry," *Proceedings of the Combustion Institute,* vol. 31, *(2),* pp. 2521-2528, 2007.
[8] T. T. Lie, *Fire and Buildings.* Barking (Ripple Rd, Barking, Essex): Applied Science Publishers Ltd, 1972.
[9] P. J. Di Nenno, *SFPE Handbook of Fire Protection Engineering (3. ed.).* Quincy, Mass: National Fire Protection Association, 2002.
[10] H. Cheng and G. V. Hadjisophocleous, "Experimental study and modeling of radiation from compartment fires to adjacent buildings," *Fire Saf. J.,* vol. 53, pp. 43-62, 2012.
[11] "Verification and validation of selected fire models for nuclear power plant applications," Federal Information & News Dispatch, LLC, Washington, 2015.
[12] U. Dundar and S. Selamet, "Fire load and fire growth characteristics in modern high-rise buildings," Fire Saf. J., vol. 135, pp. 103710, 2023.
[13] U. Wickström, *Temperature Calculation in Fire Safety Engineering.* Springer, 2016.
[14] E. D. Palik, *Handbook of Optical Constants of Solids. / II.* San Diego: Academic Press, 1998.
[15] M Salisbury, *SFES Salisbury Fire Engineering Software.* 01/06/12.
[16] R. Chitty, *External Fire Spread: Building Separation and Boundary Distances (2nd ed.).* Watford: IHS BRE Press, 2014.
[17] H. GULVANESSIAN, "EN1991 Eurocode 1: Actions on structures: Eurocodes," *Proceedings of the Institution of Civil Engineers. Civil Engineering,* vol. 144, *(2),* pp. 14-22, 2001.
[18] "BS 7974 and PD 7974 Series Kit: Fire Safety Engineering. Application of fire safety engineering principles to the design of buildings" 2019.
[19] F. Tang, L. H. Hu, M. A. Delichatsios, K. H. Lu and W. Zhu, "Experimental study on flame height and temperature profile of buoyant window spill plume from an under-ventilated compartment fire," *Int. J. Heat Mass Transfer,* vol. 55, *(1),* pp. 93-101, 2012.
[20] K. S. Goble, "Height of flames projecting from compartment openings," 2007.
[22] X. Zhang, L. Hu, M. A. Delichatsios and J. Zhang, "Experimental study and analysis on flame lengths induced by wall-attached fire impinging upon an inclined ceiling," vol. 37, *(3),* pp. 3879-3887, 2019.
[22] Y. Cui, X. Cheng, L. Gong, L. Li, H. Zhang and Y. Zhao, "Effect of Opening Geometry on the Heat Transfer Characteristics for External Flames Impinging on an Exterior Wall," *Exp. Heat Transfer,* vol. 27, *(3),* pp. 213-230, 2014.
[23] C.A. Harper, *Handbook of Building Materials for Fire Protection.* McGraw-Hill Education, 2004.
[24] F. Lugaresi, P. Kotsovinos, P. Lenk and G. Rein, "Review of the mechanical failure of non-combustible facade systems in fire," *Constr. Build. Mater.,* vol. 361, pp. 129506, 2022.